

Dynamical properties of antiferromagnetic Heisenberg spin chains

Stephan Haas, Jose Riera,* and Elbio Dagotto

*Department of Physics and Supercomputer Computations Research Institute,
Florida State University, Tallahassee, Florida 32306*

(Received 22 January 1993)

The dynamical properties of spin-1 and spin-1/2 antiferromagnetic Heisenberg chains (AHC's) are studied by diagonalizing exactly clusters of up to 18 and 26 sites, respectively. It is shown that the spin-1 AHC has a quasi-single-mode spectrum for momentum $k \geq 0.3\pi$, while the low-energy edge of the spin-1/2 AHC is dominated by a spin-wave continuum. The dispersion curve obtained for the spin-1 chain is in excellent agreement with recent experiments on $\text{Ni}(\text{C}_2\text{H}_8\text{N}_2)_2\text{NO}_2\text{ClO}_4$. The size dependence of the low-energy spectral weights is also analyzed.

I. INTRODUCTION

The quantum Heisenberg antiferromagnet is one of the simplest nontrivial models of strongly correlated electrons. However, its ground state properties are not entirely understood. In particular, the one-dimensional antiferromagnetic Heisenberg chain (AHC) has recently been given much attention both theoretically¹⁻⁹ and experimentally.¹⁰⁻¹³ This interest is mainly due to Haldane's⁶ prediction of a finite gap in the excitation spectrum of integer-spin AHC's leading to finite magnetic correlations, to be compared with the spectrum of half-odd-integer spin chains which is presumed to be gapless. Previous numerical studies for the isotropic spin-1 AHC have indeed confirmed the presence of a spin gap $\Delta_\pi \simeq 0.41J$ at $k = \pi$ and $\Delta_0 \simeq 2\Delta_\pi$ at $k = 0$, where J is the Heisenberg exchange integral.⁷ However, not much theoretical information on the *dynamical* properties of spin-1 chains is available. Carrying out such a calculation became particularly important after the recent experiments by Ma *et al.*¹⁰ on the spin-1 AHC $\text{Ni}(\text{C}_2\text{H}_8\text{N}_2)_2\text{NO}_2\text{ClO}_4$ (NENP) which have provided strong evidence of a long-lived single-mode picture in the interval $0.3\pi \leq k \leq \pi$ (the region $k \leq 0.3\pi$ is experimentally difficult to access due to the small magnetic scattering cross section in this regime). In contrast to the half-odd-integer spin chains, the dispersion curve was found to be asymmetrically displaced about $k = \pi/2$ and presents gaps for all momentum transfers.¹⁰ The integrated energy intensity drastically decreases for momentum $k < \pi/2$. Can these results be reproduced by a simple spin-1 Heisenberg model on a chain?

In this paper, the dynamical behavior of AHC's with and without spin gaps is analyzed and compared with experiments. We will study the excitation spectrum contained in the zero-temperature dynamical structure factor $S(k, \omega)$ which is proportional to the scattering cross section measured in inelastic neutron-scattering experiments¹⁰⁻¹² at low temperatures ($k_B T \ll \hbar\omega_k$). In excellent agreement with experiments, we observed that interactions between the dominant excitations are negli-

gible in this regime, leading to a single-mode spectrum in the integer-spin case above a certain threshold momentum transfer.¹⁰ For a quantitative comparison of the present numerical results with the data of Ma *et al.* it is necessary to take into account the single-ion anisotropy of NENP which is about $D \approx 0.18J \simeq 0.8$ meV.¹⁰

While relatively little is known about the dynamical properties of spin-1 chains, a vast literature on the spin-1/2 AHC is available. Static ground-state properties have been calculated using the Bethe ansatz.^{14,15} However, an exact evaluation of $S(k, \omega)$ in Bethe's framework has not been accomplished. Müller *et al.*¹ proposed an approximate expression for the dynamical structure factor which agrees well with inelastic neutron-scattering studies on KCuF_3 and $\text{CuCl}_2 \cdot 2\text{N}(\text{C}_5\text{D}_5)$.^{12,13} Recent experimental work by Nagler *et al.*¹² has nicely confirmed the existence of a spin-wave continuum with a gapless onset at the antiferromagnetic zone center ($k = \pi$) and at $k = 0$.

The Hamiltonian of the one-dimensional quantum Heisenberg antiferromagnet in the presence of single-ion anisotropy is defined by

$$H = J \sum_i \mathbf{S}_i \cdot \mathbf{S}_{i+1} + D \sum_i (S_i^z)^2, \quad (1)$$

where the sum is taken over all cluster sites, and the rest of the notation is standard. The in-plane anisotropy $E \sum_i [(S_i^x)^2 - (S_i^y)^2]$ has been neglected here. In the case of NENP it has been experimentally observed that $J \approx 3.8$ – 4.1 meV and $D \approx 0.18J$,¹⁰ while for KCuF_3 the parameters are $J \approx 17.5$ meV and $D \approx 0$.¹² D is produced by the coupling of a spin to the anisotropic orbital motion. It destroys the spin rotational symmetry of the pure Heisenberg antiferromagnet and pulls the spins into the xy plane.

We diagonalize Eq. (1) on finite clusters with periodic boundary conditions using the Lanczos algorithm.¹⁶ At $T=0$ the dynamical structure factor is given by

$$S^{\alpha\alpha}(k, \omega) = \sum_n |\langle n | S_k^\alpha | 0 \rangle|^2 \delta(\omega - (E_n - E_0)), \quad (2)$$

where $\alpha = x, y, z$, $S_k^\alpha = \frac{1}{\sqrt{N}} \sum_l e^{ikl} S_l^\alpha$, N is the num-

ber of sites, $|n\rangle$ denotes an eigenstate of H with energy E_n (E_0 being the ground-state energy), and the rest of the notation is standard. $S^{\alpha\alpha}(k, \omega)$ is extracted from its corresponding Green's function

$$S^{\alpha\alpha}(k, \omega) = -\frac{1}{\pi} \text{Im} G^{\alpha\alpha}(k, \omega), \quad (3)$$

which can be written in the form of a continued fraction^{16,17}

$$G^{\alpha\alpha}(k, \omega) = \frac{\langle 0 | (S_k^\alpha)^\dagger S_k^\alpha | 0 \rangle}{\omega - a_0 - \frac{b_1^2}{\omega - a_1 - \frac{b_2^2}{\omega - \dots}}} \quad (4)$$

The coefficients a_n and b_n are obtained from the recursive relation

$$|f_{n+1}\rangle = H|f_n\rangle - a_n|f_n\rangle - b_n^2|f_{n-1}\rangle, \quad |f_0\rangle = S_k^\alpha|0\rangle, \quad (5)$$

where Eq. (5) defines a set of orthogonal states. The coefficients are thus given by

$$a_n = \langle f_n | H | f_n \rangle / \langle f_n | f_n \rangle, \quad (6)$$

$$b_{n+1}^2 = \langle f_{n+1} | f_{n+1} \rangle / \langle f_n | f_n \rangle, \quad b_0 = 0.$$

As a check for our calculations we used the real-space correlation functions to verify that the sum rule $\int d\omega S^{\alpha\alpha}(k, \omega) = S^{\alpha\alpha}(k)$ is satisfied. Here $S^{\alpha\alpha}(k) = \sum_j \exp(-ikj) \langle 0 | S_j^\alpha S_{j+1}^\alpha | 0 \rangle$ is the corresponding static structure factor.

The convergence of lattice diagonalizations with the number of sites for the gapless excitation spectrum of the spin-1/2 AHC is slower than for the spin-1 case. Thus, finite-size effects have to be taken into account when information is extracted for the $N \rightarrow \infty$ limit. In order to reduce the size of our Hamiltonian matrix we use spin inversion, spin reflection, and the translational symmetry of Eq. (1). In spite of these simplifications the characteristic Hilbert space of the 18-site spin-1 AHC has 1227112 basis elements. The construction and diagonalization of the Hamiltonian for the $N = 18$ sites spin-1 chain demands less than an hour of CPU time on a CRAY-2 supercomputer.

II. SPIN-1 AHC

Now let us analyze the results for the spin-1 chain. Previous studies have shown^{4,7,9} that the ground state of the spin-1 AHC has zero momentum and that its spin excitation spectrum is asymmetric about $k = \pi/2$. A finite (and positive) uniaxial anisotropy splits the otherwise threefold-degenerate lowest excitation into a higher-energy $S^z = 0$ state, which we will denote as the singlet, and a lower-lying $|S^z| = 1$ doublet. In our study we will concentrate on the dynamical structure factor along the z axis which measures weights and positions of excitations in the $S^z = 0$ subspace. The splitting of the spectrum in the vicinity of $k = \pi$ due to in-plane anisotropy¹⁰ has been neglected.

In Fig. 1, we show the position of the lowest excitation energy observed in $S^{zz}(k, \omega)$ as a function of k , and compare it with the experimental results of Ma *et al.*¹⁰ The solid line is a fit to their data to the dispersion relation

$$\omega_{\parallel} = \sqrt{\Delta_{\parallel}^2 + v^2 \sin^2 k + A_{\parallel} \cos^2 \frac{k}{2}}, \quad (7)$$

where $\Delta_{\parallel} = 2.40 \pm 0.05$ meV, $v = 9.7 \pm 0.1$ meV, and $A_{\parallel} = 34 \pm 2$ meV. Our results were obtained from the exact diagonalization of $N = 16$ and $N = 18$ chains. An excellent agreement is obtained in the region $k \geq 0.3\pi$, while there is no data available below $k = 0.3\pi$. The gap at $k = 0$ is about twice the gap at $k = \pi$, which has led to the assumption that at small k we are dealing with a continuum of excitation pairs with momentum π and $-\pi$.¹⁰ In the slightly anisotropic case ($D = 0.18J$) the $k = \pi$ singlet gap is given by $0.66J$ in agreement with the results of Golinelli, Jolicoeur, and Lacaze.⁹ To show the influence of the single-ion anisotropy D in the dispersion, we have also plotted our results for the $D = 0$ case which may correspond to $A_gVP_2S_6$ where experimentally it was observed that $D/J \sim 10^{-4}$.¹⁸

The relative spectral weight of the lowest-energy excitation in $S^{zz}(k, \omega)$ as a function of the lattice size N is shown in Fig. 2(a). As $N \rightarrow \infty$, the weights of the lowest excitation peaks converge to finite values (approximately 94% for $k = \pi$). The convergence is very rapid in the vicinity of $k = \pi$, which suggests a single-mode picture in this region. On the other hand, for low-momentum transfers ($k \leq 0.3\pi$) higher-lying modes appear in the spectrum, signaling the presence of multimagnon interactions. However, the energy gap and relative peak intensity of the lowest excitation seem to remain finite in the bulk limit, even for small momentum transfer.

In Fig. 2(b), the dynamical out-of-plane structure factor of the $N = 18$ chain is shown for different momenta at $D = 0.18J$. The δ functions have been approximated by Lorentzians with a finite width $\epsilon = 0.1J$. The inte-

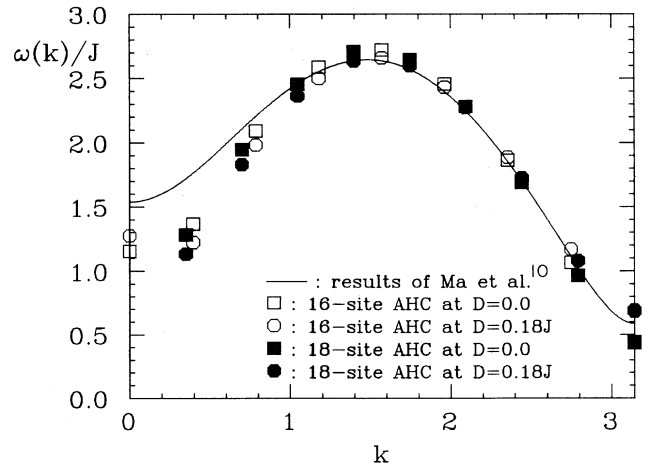


FIG. 1. Dispersion curve for a spin-1 AHC. The solid line is a fit to experimental data for NENP (Ref. 10). The symbols denote results from exact diagonalizations of 16-site and 18-site chains for anisotropies $D = 0.0$ and $D = 0.18J$, respectively.

grated spectral intensity decreases rapidly as $k \rightarrow 0$, in agreement with experiments. As shown in the figure, for $k \leq 0.3\pi$ higher-lying modes become visible, indicating the onset of a multimagnon continuum. Also, we have observed that the total spectral weight of $S^{zz}(\pi, \omega)$ also decreases as a finite single-ion anisotropy D is switched on. This indicates that the spins prefer to lie in the xy plane for positive D . Correspondingly we would expect an increase in the spectral weights of $S^{xx}(\pi, \omega)$ and $S^{yy}(\pi, \omega)$.

In Fig. 2(c), we show the first few coefficients of the continued fraction expansion for $S^{zz}(\pi, \omega)$ in the $N = 14$ and $N = 18$ chains. We observed that a truncation of the expansion beyond the first ~ 14 coefficients is possible without any noticeable change in the dynamical spectrum. It can be seen from Eq. (6) that the a_n 's carry units of energy while the b_n 's are dimensionless. The a_n 's are thus expected to grow proportional to the sys-

tem volume N , while the b_n 's should converge to a finite value as the bulk limit is approached. Both features, the scaling of a_n 's with the lattice size and the convergence of the b_n 's, are observed in Fig. 2(c). This provides evidence that the bulk limit has been already reached at $N = 18$.

We have observed that the dominant low-energy pole is isolated, and the gap to higher-lying excitations appears to persist in the bulk limit (a careful finite-size study is necessary to verify the presence of a second gap in the spectrum). Isolated poles in the spectral functions of *holes* in two-dimensional antiferromagnets are common.¹⁹ In that case, the creation of a hole causes a distortion of the background spin ground state. When the system relaxes to the new ground state, the hole still exists, but it has changed the mean values of the spins in its neighborhood, and has thus become a *dressed* hole quasiparticle. It may occur that a similar picture holds

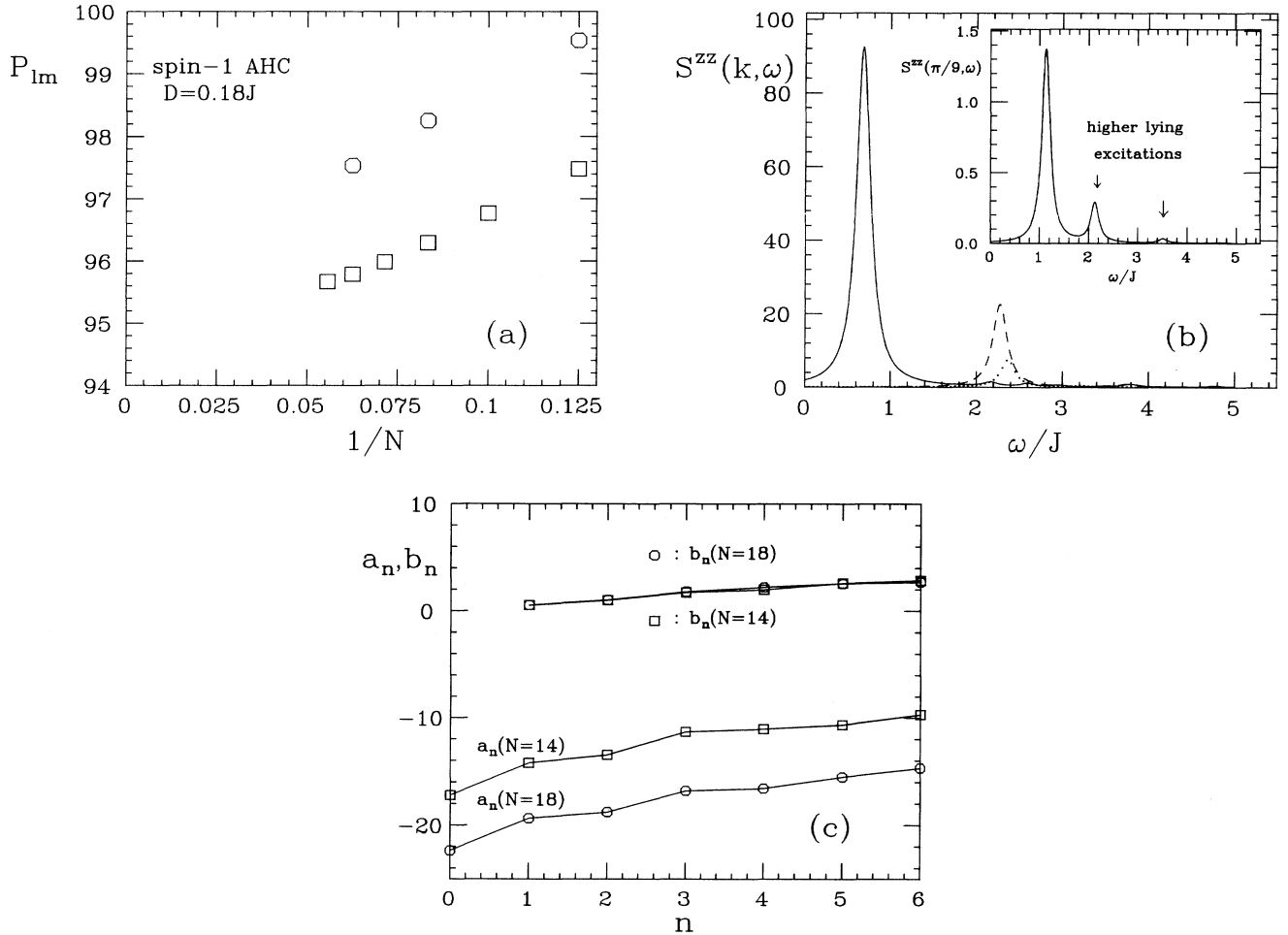


FIG. 2. (a) Volume dependence of the spectral weight of the lowest-lying excitation P_{lm} (in %) in spin-1 AHC's with up to 18 sites. Squares, $k = \pi$; octagons, $k = \pi/2$. N is the number of sites. In the limit $N \rightarrow \infty$ the spectral weights converge to finite values. (b) Out-of-plane dynamical structure factor of the $N = 18$ spin-1 AHC with single-ion anisotropy $D = 0.18J$ for different values of the momentum transfer. Solid line, $k = \pi$; dashed line, $k = 2\pi/3$; dotted line, $k = \pi/3$; inset, $k = \pi/9$. The δ functions have been given a finite width $\epsilon = 0.1J$. The inset shows that for low-momentum transfers ($k \leq 0.3\pi$) higher-lying modes are not negligible. (c) Lowest-order coefficients in the continued-fraction expansion for $S^{zz}(\pi, \omega)$. Octagons denote $N = 18$, while squares correspond to $N = 14$ spin-1 AHC.

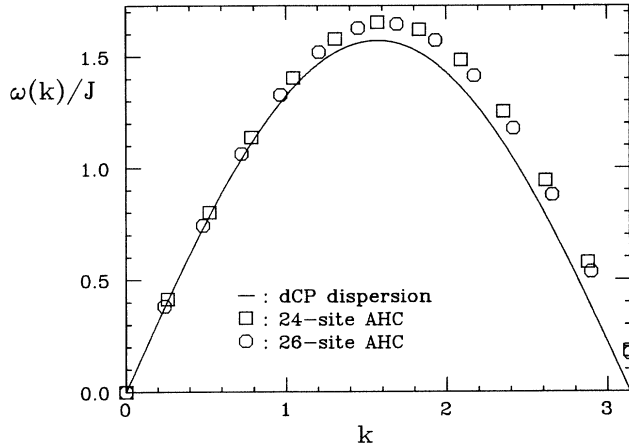


FIG. 3. Dispersion curve of a spin-1/2 AHC. The solid line is the dispersion relation proposed by des Cloiseaux and Pearson [Eq. (8)] (Ref. 15). The symbols denote results from exact diagonalizations of 24-site and 26-site chains, respectively.

for the spin-1 chain; namely, we flip a spin at a given site creating a local triplet state, and this state may relax at large times to a (still local) state not much different from the previous one; i.e., only its spin neighbors are altered. We are currently investigating this possibility.

III. SPIN-1/2 AHC

The spin-1/2 chain has been studied extensively,^{1-3,7,12-15} and there are approximate analytical expressions available for some dynamical observables. The onset of the excitation spectrum of a spin-1/2 AHC is given by the des Cloiseaux-Pearson dispersion¹⁵

$$\omega_k^l = \frac{\pi J}{2} |\sin(k)|, \quad (8)$$

which is gapless at $k = \pi$ and 0. Comparing our data in Fig. 3 for the lowest excitations of a $N = 26$ chain with

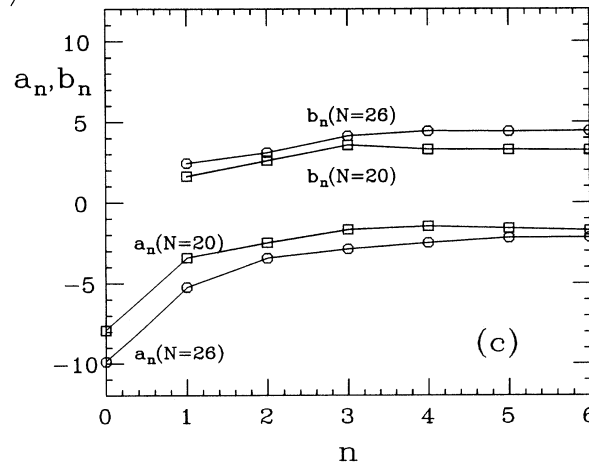
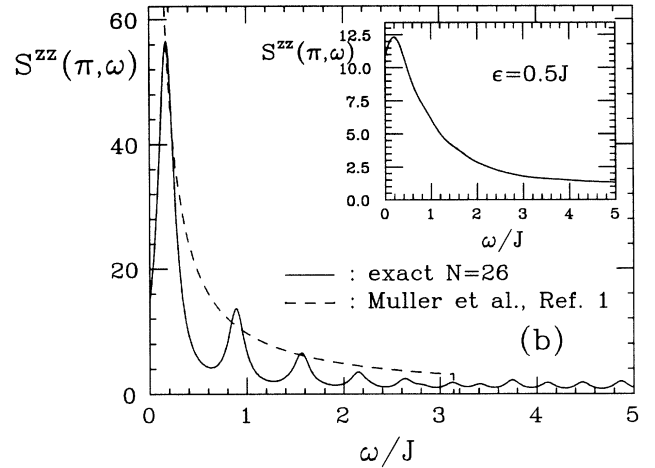
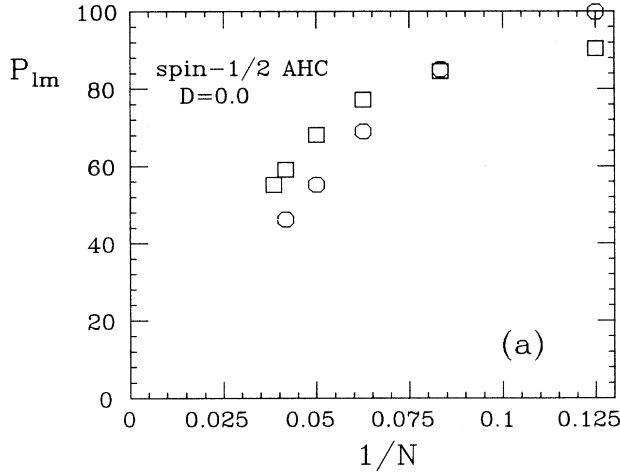


FIG. 4. (a) Volume dependence of the spectral weight P_{lm} (in %) of the lowest-lying excitations in spin-1/2 AHC's with up to 26 sites. Squares, $k = \pi$; octagons, $k = \pi/2$. N is the number of sites. In the bulk limit these weights seem to vanish. (b) Out-of-plane dynamical structure factor for a $N = 26$ spin-1/2 AHC (solid line) at $k = \pi$. The δ functions have been given a finite width $\epsilon = 0.1J$. The dashed line is a fit to an approximate analytical expression Eq. (10) by Müller *et al.* (Ref. 1). The inset shows the same dynamical spectrum with broadened peaks ($\epsilon = 0.5J$). (c) Lowest-order coefficients in the continued-fraction expansion for $S^{zz}(\pi, \omega)$. Octagons denote $N = 26$, while squares correspond to $N = 20$ spin-1/2 AHC.

Eq. (8) we find good agreement. The small gap at $k = \pi$ is due to the finite size of our chain and vanishes in the bulk limit.¹⁷ In contrast to the massive spin-1 AHC, the spectrum is now symmetrical about $k = \pi/2$.

Above this lower boundary [Eq. (8)], there is a continuum of excitations which is believed to be made out of pairs of spinons² with momenta between 0 and $k/2$. The upper boundary of this continuum is given by

$$\omega_k^u = \pi J |\sin(k/2)|. \quad (9)$$

Based on the selection rules and their exact dispersion curves Müller *et al.*¹ have proposed the following approximate expression for the out-of-plane dynamical structure factor:

$$S^{zz}(k, \omega) = \frac{A}{\sqrt{\omega^2 - \omega_k^l{}^2}} \Theta(\omega - \omega_k^l) \Theta(\omega_k^u - \omega), \quad (10)$$

where A is a constant and $\Theta(x)$ is a cutoff step function. The upper cutoff at ω_k^u was introduced to guarantee that the usual sum rules are satisfied. It may be interpreted as the maximum energy of a spinon pair. However, higher-order scattering processes result in small contributions above this boundary which are observed in exact diagonalizations of finite clusters. Thus, Eq. (9) should not be interpreted as a rigorous sharp upper bound for the spectrum.

To compare these predictions with numerical results, the intensities of the lowest-lying peaks in $S^{zz}(k, \omega)$ are shown for different momentum transfers in Fig. 4(a). In contrast to the spin-1 chain the spectral weights of these peaks seem to vanish in the bulk limit. This clearly indicates that now we are dealing with a spinon pair continuum as opposed to a single-mode spectrum as in the spin-1 case. As expected, finite-size effects play a more important role in the gapless half-odd-integer AHC's than in a massive theory, as can be seen in our plot of $S^{zz}(\pi, \omega)$ [Fig. 4(b)]. Although the smaller Hilbert space of spin-1/2 chains allows us to easily diagonalize systems of 26 sites, the results still show finite-size effects. Actually, we expect that the peaks observed in the spectrum will

merge into a continuum increasing the size of the lattice. A combination of several boundary conditions may alleviate this problem. Nevertheless, there is good qualitative agreement between Eq. (10) and the numerical results. The inset of Fig. 4(b) shows $S^{zz}(\pi, \omega)$ where the occurring poles have been approximated by Lorentzians with a large width $\epsilon = 0.5J$. The artificially broadened dynamical spectrum has the $1/\omega$ behavior proposed by Müller, and this is roughly the result we expect in the bulk limit when more poles converge into a continuous spectrum.

In Fig. 4(c), the first 11 coefficients in the continued-fraction expansion for $S^{zz}(\pi, \omega)$ are shown for the $N = 20$ and $N = 26$ chains. In contrast to the spin-1 case the b_n 's have not converged, indicating that the bulk limit has not been reached as expected. Note that for easy comparison of the convergence in Fig. 2(c) and Fig. 4(c) we have chosen cluster sizes which render similar ratios, i.e., $14/18 \approx 20/26$.

In summary, the dynamical behavior of spin-1/2 and spin-1 AHC's has been studied using numerical techniques. Our data suggest that a single-mode approximation is adequate above $k = 0.3\pi$ for the massive spin-1 AHC in agreement with recent experiments by Ma *et al.*¹⁰ From the dynamical structure factor and the scaling of spectral weights with cluster size in the spin-1/2 AHC, we infer the existence of a spin-wave continuum, in contrast to the spin-1 AHC case.

We recently became aware of work by O. Golinelli, T. Jolicoeur, and R. Lacaze,²⁰ and by M. Takahashi²¹ with results for the spin-1 chain similar to ours.

ACKNOWLEDGMENTS

We thank S. Nagler, T. Jolicoeur, and A. Moreo for useful discussions. The support of the Supercomputer Computations Research Institute (SCRI) is acknowledged. The computer calculations were carried out on the CRAY-2 at the National Center for Supercomputing Applications, Urbana, Illinois, and on the CRAY-YMP at Florida State University.

* Present address: Physics Division and Center for Computationally Intensive Physics, Oak Ridge National Laboratory, Oak Ridge, TN 37831-6373.

¹ G. Müller *et al.*, Phys. Rev. B **24**, 1429 (1981), and references therein.

² L.D. Fadeev and L.A. Takhtajan, Phys. Lett. **85A**, 375 (1981).

³ J.B. Parkinson and J.C. Bonner, Phys. Rev. B **32**, 4703 (1985); J. Borysowicz, T.A. Kaplan, and P. Horsch, *ibid.* **31**, 1590 (1985).

⁴ A. Moreo, Phys. Rev. B **35**, 8562 (1987); **36**, 8582 (1987); F. Alcaraz and A. Moreo, *ibid.* **46**, 2896 (1992).

⁵ Dynamical results for spin chains have been presented by J. Deisz, M. Jarrel, and D.L. Cox, Phys. Rev. B **42**, 4869 (1990), using the maximum-entropy method. These results were obtained at finite temperature and with the guidance

of a default model. Although the broadening intrinsic to the maximum-entropy method prevents a detailed comparison with our exact results for smaller chains, in general we observed an overall good qualitative agreement.

⁶ F.D.M. Haldane, Phys. Rev. Lett. **50**, 1153 (1983); Phys. Lett. **93A**, 464 (1983).

⁷ M. Takahashi, Phys. Rev. Lett. **62**, 2313 (1989); T. Sakai and M. Takahashi, Phys. Rev. B **42**, 1090 (1990); M. Takahashi, *ibid.* **38**, 5188 (1988).

⁸ M.P. Nightingale and H.W. Blöte, Phys. Rev. B **33**, 659 (1986).

⁹ O. Golinelli, T. Jolicoeur, and R. Lacaze, Phys. Rev. B **45**, 9798 (1992).

¹⁰ S. Ma *et al.*, Phys. Rev. Lett. **69**, 3571 (1992).

¹¹ W.J.L. Buyers *et al.*, Phys. Rev. Lett. **56**, 371 (1986); Z. Tun *et al.*, Phys. Rev. B **42**, 4677 (1990).

- ¹² S.E. Nagler *et al.*, Phys. Rev. B **44**, 12361 (1991); S.E. Nagler *et al.*, J. Magn. Magn. Mater. **102-107**, 847 (1992).
- ¹³ R.A. Cowley *et al.* (unpublished).
- ¹⁴ H.A. Bethe, Z. Phys. **71**, 205 (1931).
- ¹⁵ J. des Cloiseaux and J.J. Pearson, Phys. Rev. **128**, 2131 (1962).
- ¹⁶ E. Dagotto, Int. J. Mod. Phys. B **5**, 907 (1991), and references therein.
- ¹⁷ E.R. Gagliano and C.A. Balseiro, Phys. Rev. Lett. **59**, 2999 (1987). See also *The Recursion Method and Its Applications*, edited by D.G. Pettifor and D.L. Weaire (Springer, Berlin, 1985).
- ¹⁸ H. Mutka *et al.*, Phys. Rev. Lett. **67**, 497 (1991).
- ¹⁹ E. Dagotto *et al.*, Phys. Rev. B **41**, 9049 (1990).
- ²⁰ O. Golinelli, T. Jolicoeur, and R. Lacaze, J. Phys. C **5**, 1399 (1992).
- ²¹ M. Takahashi, Phys. Rev. B **48**, 311 (1993).